Dispersion and Modulation of the Linear Optical Properties of GaAs–AlAs Superlattice Waveguides Using Quantum-Well Intermixing

T. C. Kleckner, A. S. Helmy, *Member, IEEE*, K. Zeaiter, David C. Hutchings, *Senior Member, IEEE*, and J. S. Aitchison, *Senior Member, IEEE*

***Abstract*—We report on the large modulation of the optical properties of a 14:14 monolayer GaAs–AlAs superlattice waveguide following quantum-well intermixing. Low-temperature photoluminescence measurements illustrate a large 169-meV differential blue-shift obtained between the disordering-suppressed and disordering-enhanced materials. Effective index measurements are presented as a function of polarization, for both the as-grown and disordered material for near-bandedge and half-bandedge wavelengths, which is the wavelength range 775–1550 nm. The largest effective refractive index shift observed was 9×10^{-2} which exceeds that previously reported for disordered AlGaAs ternary multilayer structures, and illustrates the potential of the superlattice for the fabrication of etch-free, planar optical components with large index contrast.**

***Index Terms*—Frequency conversion, integrated optics, nonlinear optics, optical waveguides, quantum well intermixing, quasi-phase matching (QPM), second-harmonic generation, semiconductor waveguides.**

I. Introduction

THE III–V semiconductor has become widely used in integrated optoelectronic circuits and nonlinear optical devices. In particular, mature growth, lithography and etching technologies allow the fabrication of low-loss guiding structures and the use of electronic-scale heterostructures enables additional control, flexibility and functionality to be incorporated at the device design stage. There are currently a number of techniques for patterning the compositional structure of an optical chip, including etch and regrowth, selective area growth [1] and quantum-well intermixing [2], [3]. Although these techniques were initially developed to define low-loss interconnects between active devices (i.e., modification of the absorption and gain: $\mathrm{Im}\chi^{(1)}$), they also provide the means to pattern the refractive index $(\mathrm{Re}\chi^{(1)})$ [4], [5] and nonlinear optical coefficients ($\chi^{(2)}$ and $\chi^{(3)}$) [6]. Applications of refractive index patterning include the definition of waveguide regions [7], [8] or Bragg gratings. In addition, modulation of the second-order susceptibility provides a route to realizing quasi-phase-matching (QPM) structures for frequency conversion [9], [10], which take advantage of the large nonlinear coefficient (figure of merit d^2/n^3 is around 10 times larger than that of periodically-poled $\mathrm{LiNbO_3}$) and the extended midinfrared transparency range in comparison to conventional ferroelectric media.

Provided the optical frequency does not correspond to absorption or gain resonances, the effect on the optical coefficients from single or few quantum-well layers is rather small due to the limited overall volume fill fraction of the well material. Therefore, in order to maximize the modulation in either the effective refractive index of the guided modes, or the nonlinear optical coefficients, quantum-well layers should be relatively closely spaced and the heterostructure region should have a substantial overlap with the guided modes. This requirement is most straightforwardly satisfied with a superlattice structure forming the core of a waveguide. A theoretical analysis of GaAs–AlAs superlattice structures has been previously performed for second-order [11] and third-order [12] nonlinearities which indicate a substantial modulation in the bulk-like coefficients can be obtained between an as-grown and intermixed structure. In particular, a 14:14 monolayer GaAs–AlAs superlattice was identified as near optimal for second-harmonic (SH) generation with a 1550-nm fundamental, or equivalently near degenerate parametric processes with a 775-nm pump.[13]

There is therefore a requirement for a comprehensive characterization of the refractive index in such superlattice structures and the subsequent modifications under intermixing. Current models for refractive index provide, at best, a second-decimal point accuracy which is insufficient for the proper design of devices that rely on Bragg gratings, or QPM structures [14], [15] The reasons for this characterization are two-fold. First, a knowledge of the refractive index modification, including the birefringence, and resolution are required for the design of linear optical components such as waveguides and Bragg gratings. Second, for frequency conversion applications the dispersion of the refractive index is required across a substantial wavelength range, in order to determine the coherence length and hence the QPM period. The narrow bandwidth of the QPM process requires a detailed knowledge of the refractive index to a relatively high degree of precision. Furthermore a

Manuscript received September 30, 2005; revised November 11, 2005. The work of T. C. Kleckner was supported in part by NSERC Canada and the Association of Commonwealth Universities and the British Council in the form of a Commonwealth Scholarship. The work of D.C. Hutchings was supported in part by a Royal Society of Edinburgh/Scottish Executive Support Research Fellowship.

T. C. Kleckner is with Lumerical Solutions, Inc. Vancouver, BC V6C 1H2, Canada.

A. S. Helmy and J. S. Aitchison are with the Edward S. Rodgers Department of Electrical and Computer Engineering, University of Toronto, Toronto, ON M5S 3G4, Canada (e-mail: a.helmy@utoronto.ca).

K. Zeaiter is with Spheral Solar Power Inc., Cambridge ON N3H 5M2, Canada.

D. C. Hutchings is with the Department of Electronics and Electrical Engineering, University of Glasgow, Glasgow G12 8QQ, U.K.

Digital Object Identifier 10.1109/JQE.2005.864155

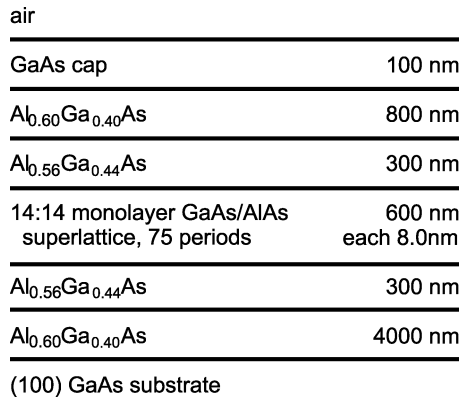

Fig. 1. Schematic with the details of the epitaxial structure used in this work.

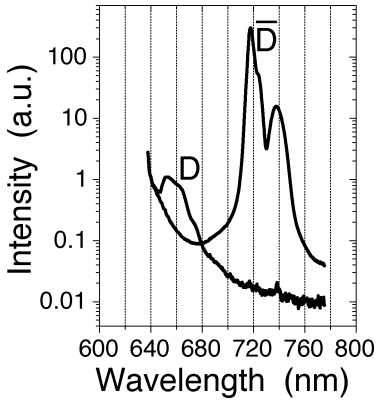

Fig. 2. Low-temperature (10 K) PL measurements of disordered (D) and disordering-inhibited $(\overline{D})$ superlattice material annealed at a temperature of 750 °C for 60 s.

refractive index grating can provide Bragg scattering and can, by itself, also contribute to the QPM process. [16] Calculations indicate that for the present experimental structures, the relative phase relationship between the two QPM processes can compromise the frequency conversion process [17], [18] An accurate knowledge of the refractive index potentially allows the minimization of optical losses due to Bragg scattering and the minimization of the competition between the different QPM processes.

In this paper we present results from a comprehensive study of the linear optical properties of the as-grown and disordered superlattice structures. For the data to be useful, we need to maximize the accuracy in the determination of the effective index of a slab waveguide, with the superlattice forming the core layer. The refractive index measurement setup is based on grating coupled slab waveguide structures, providing an accuracy of 1×10^{-4} in the refractive index measured.

II. Photoluminescence Measurements and Quantum-Well Intermixing

The sample used in these experiments was grown by molecular beam epitaxy (MBE) on to a GaAs substrate and is shown schematically in Fig. 1. The details of the structure have been previously published [10]. The 600-nm-thick superlattice waveguide core consisted of 75 periods of 14:14 monolayer (4.0:4.0 nm) GaAs–AlAs layers and is clad on either side with 300 nm 56% AlGaAs layers; these cladding layers have been added to the structure to improve end-fire coupling efficiencies [13]. The epilayers were grown at an elevated substrate temperature to ensure good optical quality of the resulting waveguide structure. Preparation of the photoluminescence sample began with the deposition of 500 nm of PECVD SiO_2 over the entire sample surface. The sample was spun with a 0.9-μm-thick UV3 resist and areas to be intermixed were defined through exposure to 50 kV electrons at an exposure dose of 20 μC/cm^2. Following development, the pattern was transferred to the underlying 500-nm-thick SiO^2 layer through reactive ion etching in a CHF_3 plasma and the UV3 resist was subsequently removed in an O_2 plasma. Disordering of the superlattice relied upon point defect generation through sputtered-silica deposition [19]. In the areas protected by the 500-nm-thick PECVD SiO_2 layer the disordering process was suppressed while those areas exposed to sputtered silica were disordered. Following sputtering, the sample was placed between two pieces of bulk GaAs to prevent As desorption and annealed in a rapid thermal annealer at 750 °C for a duration of 60 s.

Photoluminescence spectra measured at 10 K for bulk-area disordered (D) and disordering-suppressed $(\overline{D})$ regions are shown in Fig. 2. The rise of the photoluminescence signal at short wavelength is the result of the 632.8-nm excitation wavelength of the HeNe source used. As illustrated, a 169-meV shift of the photoluminescence peak is achieved between the (D) and $(\overline{D})$ samples. Compared to data measured for single and double quantum wells [20], [21], and other multiple quantum-well and superlattice structures [22], [23], the large energy shift of the present data is indicative of the ease with which the thin superlattice layers are disordered and the extent to which the band structure of the binary structure investigated is modulated upon disordering. It is worth noting that the large 169-meV blue-shift achieved in the present work was at a much lower temperature 750 °C compared to the 900 °C and 800 °C used to achieve shifts of 140 [23] and 100 meV [22], respectively. The 47-meV energy detuning between the main superlattice peak and the small peak on the low energy side in the $(\overline{D})$ sample is in excellent agreement with longitudinal optical (LO) phonon energies in the AlAs layers [24], [25]. The large decrease in photoluminescence intensity upon disordering is partially attributed to the nature of the superlattice structure investigated to undergo a transition from a direct- to indirect-gap upon disordering. Indeed, increasing the temperature beyond 750 °C results in further suppression in the photoluminescence (PL) peak as the process of complete intermixing of the structure to the average (indirect) alloy is approached. The spatial resolution of the process has been studied and was found to be on the order of 1 μm.

III. Refractive Index Measurements

The waveguide effective index was measured using the grating coupling technique. The grating couplers were designed for nominal coupling angles of 30° using the AlGaAs refractive index model of Afromowitz and assuming the index of the superlattice was approximated by a 50% AlGaAs alloy [14]. The measurements were performed using the both a

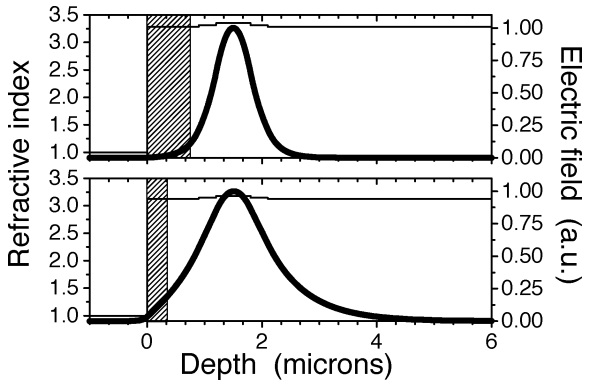

Fig. 3. Field profiles within the structure shown in Fig. 1. The hatched regions illustrate the extent to which the etched grating coupler perturbs shows the extent to which the waveguide mode is perturbed for a near-bandgap wavelength of 775 nm (top panel) and a half-bandgap wavelength of 1550 nm (bottom panel).

solid-state titanium-sapphire laser tunable from 770 to 880 nm and an external-cavity laser diode emitting in the range from 1460 to 1580 nm.

To facilitate fabrication, a 560-nm period first-order grating was chosen for the half-bandgap wavelengths, and an 840-nm period third-order grating was chosen for near-bandgap wavelengths. Two-dimensional mode solver predictions were used to design the etch depths of the grating coupler for minimum perturbation of the optical mode. This resulted in etch depths of 800 and 300 nm being selected for the bandgap and half-bandgap grating couplers which resulted in estimated effective index perturbations on the order of 6×10^{-4} and 8×10^{-4}, respectively. Grating couplers were fabricated on as-grown material and disordered material produced through sputtering of 50 nm of SiO_2 and subsequent annealing at 750 °C for 60 s. Fig. 3 depicts the field profiles in the etched grating coupler region indicating the extent of the perturbation of the waveguide mode for a near-bandgap wavelength of 775 nm (top panel) and a half-bandgap wavelength of 1550 nm (bottom panel). Following disordering, all samples were cleaned and coated with a 150-nm-thick plasma-enhanced chamical vapor deposition (PECVD) SiO_2 layer. Grating regions of 400×400 μm^2 were defined through exposure of a 200-nm-thick 4% - 4% polymethyl methacrylate (PMMA) bilayer, electron-beam resist exposed to 50-kV electrons at doses of 400 μC/cm^2. Intermediate pattern transfer into the silica layer took place in a CHF_3 etch after which the PMMA resist was removed in an O_2 plasma. Final pattern transfer to the designed depths of 300 and 800 nm took place through reactive ion etching in a $SiCl_4$ plasma.

The samples were mounted vertically upon a temperature controlled block maintained at 25 °C $\pm$ 0.01 °C, sufficient to maintain temperature-induced refractive index variations on the order of 1×10^{-5} [26], as can be seen in te schematic in Fig. 4(a). This mount was placed on a computer-controlled stepper motor driven rotational stage accurate to within 0.001 deg. Radiation from the lasers passed through a wave-plate and a polarizing beam-splitting cube to facilitate measurements for both the TE and TM polarization data. The strength of the mode transmitted through the cleaved facet of the sample was measured as a function of incidence angle. As explained by Dakss *et al.* in their

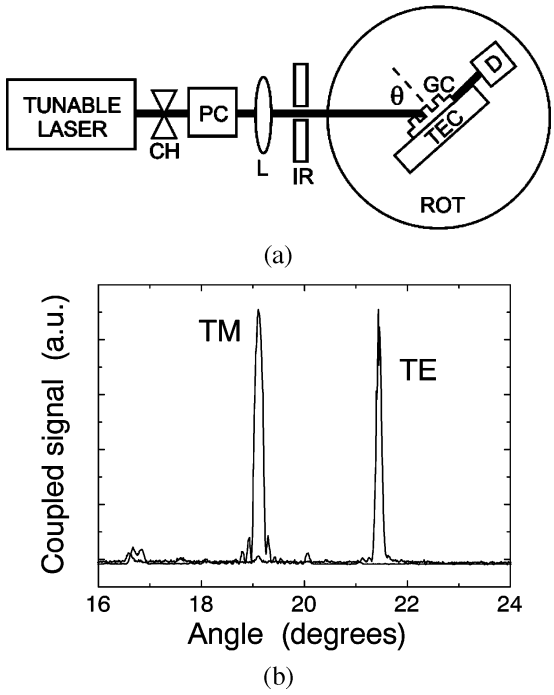

Fig. 4. Schematic in (a) shows the refractive index measurement setup. Temperature controlled (TEC) grating coupler (GC) is mounted on a computer controlled rotation stage (ROT) accurate to 0.001°. The optical chopping is used to enhance the sensitivity of the detector (D), while the polarization control (PC) enables the measurement of both TE and TM. The use of a lens with a focal length (L) of 150 cm was to facilitate beam positioning. (b) Shows and example of the signal quality of the coupling resonances acquired by the grating coupler measurement setup for the as-grown superlattice sample.

original work on the grating coupler [27], the waveguide effective index N can be related to the coupling angle such that

$$\sin(\theta_c) = N - \nu\lambda/\Lambda$$

where ν represents the grating harmonic, λ is the free-space wavelength of radiation, and Λ is the period of the grating coupler. The mode profiles for the measured resonances were checked to ensure that the lowest order mode was being excited. Similar to previous reports [26], [27], [29], the measured full-width at half-maximum (FWHM) of the coupling resonances was on the order of 0.1 degree. The nominal coupling angle is estimated via Gaussian regression and suggests an error in determining the coupling angle of 6×10^{-4} degrees. However, the nominal coupling angle shown in Fig. 4(b) must be referenced to the surface normal, as established via retro-reflection of the incident beam through a 100-μm aperture at a distance of 30 cm from the sample face. The quadrature sum of these two errors results in overall angle determination on the order of 2×10^{-2} degrees. Contrary to previous work where it is assumed that the surface normal is determined exactly [28], [29], we conclude that the error resulting from retro-reflection of the incident beam through an aperture is more significant than the measurement of the unreferenced coupling angle itself. This can be compared to the 2-deg. difference in peak position due to the natural birefringence of the sample.

Taken together the high-precision electron beam lithography which defines periodic structures with a fractional error in period of 1×10^{-4}, and including an estimate to address the extent

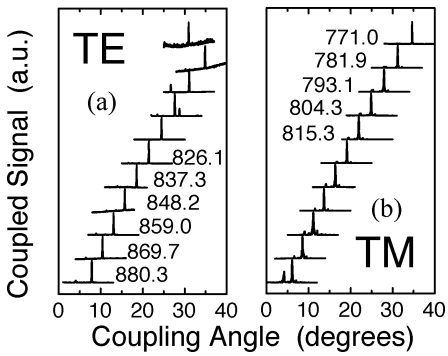

Fig. 5. Evolution of grating coupler signal with wavelength for both input polarizations. The gradual degradation of the signal-to-noise ratio as the measurements extend to shorter wavelengths can be attributed to increased waveguide confinement at shorter wavelengths and a decreasing overlap of the waveguide mode with the etched surface grating.

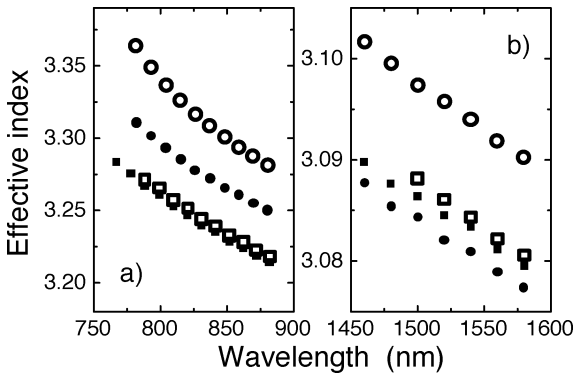

Fig. 6. (a) Near-bandgap and b) half-bandgap dispersion of effective refractive indexes for both the as-grown (circular symbols) and disordered material annealed at 750 °C for 60 s (square symbols). The open symbols denote TE polarization while the filed symbols denote TM polarization.

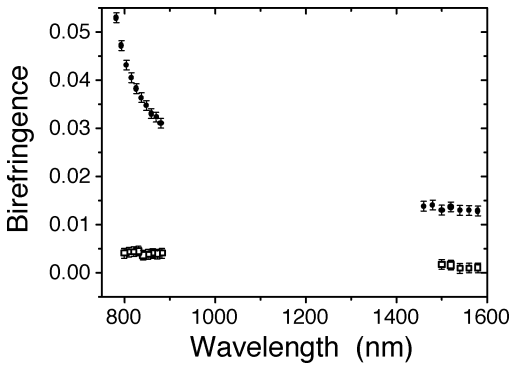

Fig. 7. Shown is the measured birefringence of the effective refractive index data for both as-grown (filled circles) and disordered material (squares).

to which the grating perturbs the waveguide core, the waveguide effective index can be determined with typical accuracies of approximately 9×10^{-4}.

Coupling measurements were carried out as a function of wavelength in order to determine the dispersion of the refractive index of the superlattice waveguide. Fig. 5 shows measured coupling resonances for: a) TE and b) TM polarized inputs, measured for the as-grown superlattice for near-bandedge wavelengths. Note the greater than 20 degrees variation in coupling angle over the wavelengths measured, which is further indication of the high sensitivity attainable with this type of measurement. Especially evident for the TE polarization in part (a) of Fig. 5 is gradual degradation of the signal-to-noise ratio as the measurements extend to shorter wavelengths. This signal-to-noise degradation results from increased waveguide confinement at shorter wavelengths and a decreasing overlap of the waveguide mode with the etched surface grating. This effect has a maximum at the shortest wavelength tested where, for the TE polarization, the incoming radiation couples to a higher order mode verging on cutoff and fails to couple to the fundamental waveguide mode. This demonstrates the minimal extent to which the grating coupler perturbs the waveguide core, and further provides confirmation of the accurate nature of the measured data.

Using equation 1 to convert the angular data to effective index data, Fig. 6 shows the (a) near-bandgap and (b) half-bandgap dispersion of effective refractive indexes for both the as-grown and disordered material. Disordering the current structure, itself optimized for the maximum modulation in optical properties upon disordering, provides changes in near-bandgap effective refractive index for the TE and TM mode of 9×10^{-2} and 4×10^{-2}, respectively. The previous largest reported index change of $\Delta n = 8.36 \times 10^{-2}$ achieved in zinc induced disordered material [4].

IV. Discussion

Overall, the substantial modulation in effective refractive index attainable in the current structure upon disordering modulation is sufficient to support guided-waves. The demonstration of quasi-phase-matched SH generation indicates that submicron resolution can be obtained using ion-implantation induced disordering [10]. Hence, there is the potential to fabricate various waveguide devices, e.g., splitters, couplers, ring structures and interferometers, without etching. In many respects this is equivalent to ion-exchange methods for writing waveguide devices in dielectrics and has the similar advantage of reducing scattering losses in comparison to etched waveguide walls which usually incorporate some degree of roughness, more significant for deep and dry etching. Using this disordering method for the modification of the refractive index can be applied to both passive and active devices. The post growth nature of the technique offers both flexibility and simplicity compared to methods where the integration is incorporated during the wafer growth. Particularly important for the Al containing compounds, is avoiding the technological difficulties associated with etch and over-growth of heterostructures due to the oxidation of Al.

There is also a significant polarization dependence of the modification of the index upon disordering allowing polarization selective functionality to be incorporated into devices. Fig. 7 shows the measured birefringence of the effective refractive index data for both as-grown and disordered material. Especially evident, and in agreement with previous observations, is the strong relaxation of the superlattice birefringence upon disordering. This birefringence modulation can also be used in conjunction with nonlinear optical effects utilizing $\chi^{(2)}$ or $\chi^{(3)}$ for novel applications [31]. Superlattice structures also possess

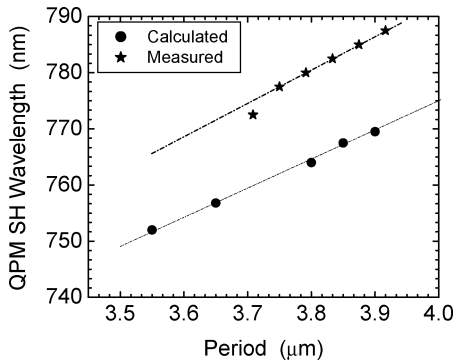

Fig. 8. Measured QPM wavelength versus period compared with the calculated values based on the refractive index measurements conducted in this work. The slope of the calculated values, which is in units of nanometer of QPM SH wavelength per micrometer of QPM period, is 52 nm/μm while that of the measured data is 68 nm/μm.

a large anisotropic contribution to the polarization dependence of the nonlinear optical coefficients ($\chi^{(2)}$ and $\chi^{(3)}$) and similarly disordering leads to a much diminished anisotropy, although a substantial anisotropic component remains in the nonlinear coefficients (but not in the material component of the linear optical coefficients) due to the underlying zinc-blende crystal structure [12].

Knowledge of the refractive index at the relevant wavelengths and its modification upon disordering allows the determination of the appropriate QPM period for a given frequency conversion process. In Fig. 8, the calculated periods for type I phase matching, based on the current slab waveguide measurements, are plotted versus the corresponding QPM SH wavelength. For comparison we also show recent tuning curve results indicating the wavelength for the maximum SH generation for various QPM periods in a strip-loaded waveguide fabricated in a nominally identical wafer [30]. As can been seen from the figure both plots have a similar slope, but the absolute QPM periods obtained for a particular SH peak wavelength in the strip-loaded waveguide are approximately 0.3 μm shorter than that inferred from the current slab waveguide measurements. We attribute this offset to the different guiding structure (two-dimensional for the strip-loaded versus one-dimensional for slab), which will result in a further modification to the effective index, and possible unintentional differences in the MBE growth between the two nominally identical wafers. However it is reassuring to see the slope of both tuning curves match as the slopes are dominated by the material dispersion. The results here can be extended to determine tuning curves for nondegenerate cases which are appropriate for difference frequency generation and parametric processes.

The large change in refractive index observed here is attributed to the near complete intermixing of the short period binary superlattice structure, indicated by the correspondingly large bandgap shift of $\sim$170 meV, and not to the specific intermixing method used. This substantial refractive index modulation has implications for QPM using domain disordering. A refractive index modulation can also be used for quasi-phase-matching second-order interactions [16] and careful consideration is required when both the modulation in the linear and nonlinear coefficients contribute to the frequency conversion process. In the transparency window of semiconductors, the increase in the fundamental absorption edge energy upon disordering provides a reduction in magnitude of both the effective index and the nonlinear coefficient $\chi^{(2)}$. For the case of second-harmonic generation, the relative phase of the generated SH wave is opposite for these two contributions, compromising achievable conversion efficiencies. Accurate knowledge of the modulation in coefficients allows the use of detailed simulations to provide an estimation of the reduction in efficiency [17], [18] and the investigation into device designs to minimize the problem. Similarly applications based on the modulation of $\chi^{(3)}$ (for example spatial soliton emission [31]) will equally have to take account of the beneficial or detrimental effects resulting from the associated refractive index modification.

V. Conclusion

In this work, we measured large modulation in the refractive index obtained for quantum-well intermixing of a 14:14 monolayer GaAs–AlAs superlattice. Low-temperature photoluminescence measurements indicate a large 169 meV differential blue-shift obtained between disordering-suppressed and disordering-enhanced material. Effective index measurements are presented as a function of polarization, for both as grown and disordered material for near-bandedge and half-bandedge wavelengths. The largest effective refractive index shift observed 9×10^{-2} exceeds previous reports for disordered AlGaAs ternary multilayer structure. This value suggests that the superlattice structure has potential applications for the direct fabrication of integrated optical waveguides, integrated splitters, and interferometers. The birefringence modulation measured is also useful for device fabrication given the ease by which the spatial modulation of this dispersion can be achieved. The comprehensive nature of the measurements reported will serve as a valuable design tool for active and passive components aimed to operate around 1550 nm.

References

[1] J. J. Coleman, R. M. Lammert, M. L. Osowski, and A. M. Jones, "Progress in InGaAs-GaAs selective-area MOCVD toward photonic integrated circuits," *IEEE J. Sel. Topics Quantum Electron.*, vol. 3, no. 3, pp. 874–884, Jun. 1997.

[2] E. H. Li, E. S. Koteles, and J. H. Marsh, "Interdiffused quantum-well materials and devices," *IEEE J. Sel. Topics Quantum Electron.*, vol. 4, no. 4, p. 581, Jul. 1998.

[3] J. H. Marsh, "Quantum-well intermixing," *Semicond. Sci. Technol.*, vol. 8, pp. 1136–1155, 1993.

[4] S. I. Hansen, J. H. Marsh, J. S. Roberts, and R. Gwilliam, "Refractive index changes in a GaAs multiple quantum well structure produced by impurity-induced disordering using boron and fluorine," *Appl. Phys. Lett.*, vol. 58, pp. 1398–1400, 1991.

[5] S.-K. Han, S. Sinha, and R. V. Ramaswamy, "Effect of zinc impurity induced disordering on the refractive index of GaAs–AsGaAs multi-quantum wells," *Appl. Phys. Lett.*, vol. 64, pp. 760–762, 1994.

[6] J. S. Aitchison, C. J. Hamilton, M. W. Street, N. D. Whitbread, D. C. Hutchings, J. H. Marsh, G. T. Kennedy, and W. Sibbett, "Control of the second- and third-order nonlinearities in GaAs-AlGaAs multiple quantum wells," *Pure Appl. Opt.*, vol. 7, pp. 327–333, 1998.

[7] T. Wolf, C.-L. Shieh, R. Engelmann, K. Alavi, and J. Mantz, "Lateral refractive index step in GaAs–AlGaAs multiple quantum well waveguides fabricated by impurity-induced disordering," *Appl. Phys. Lett.*, vol. 55, pp. 1412–1414, 1989.
[8] J. Haysom, A. Delage, J. He, E. S. Koteles, P. J. Poole, Y. Feng, R. D. Goldberg, I. V. Mitchell, and S. Charbonneau, "Experimental analysis and modeling of buried waveguides fabricated by quantum-well intermixing," *IEEE J. Quantum Electron.*, vol. 35, no. 9, pp. 1354–1363, Sep. 1999.
[9] A. Saher Helmy, D. C. Hutchings, T. C. Kleckner, J. H. Marsh, A. C. Bryce, J. M. Arnold, C. R. Stanley, J. S. Aitchison, C. T. A. Brown, K. Moutzouris, and M. Ebrahimzadeh, "Quasi phase matching in GaAs-AlAs superlattice waveguides via bandgap tuning using quantum well intermixing," *Opt. Lett.*, vol. 25, pp. 1370–1373, 2000.
[10] K. Zeaiter, D. C. Hutchings, R. Gwilliam, K. Moutzouris, S. V. Rao, and M. Ebrahimzadeh, "Quasiphase matched second harmonic generation in GaAs–AlAs superlattice waveguide using ion-implantation induced intermixing," *Opt. Lett.*, vol. 28, pp. 911–913, 2003.
[11] D. C. Hutchings, "Modulation of the second-order susceptibility in GaAs–AlAs superlattices," *Appl. Phys. Lett.*, vol. 76, pp. 1362–1364, 2000.
[12] ——, "Theory of ultrafast nonlinear refraction in semiconductor superlattices," *IEEE J. Sel. Topics Quantum Electron.*, vol. 10, no. 1, p. 1124, Jan. 2004.
[13] D. C. Hutchings and T. C. Kleckner, "Quasi phase matching in semiconductor waveguides by intermixing; optimization considerations," *J. Opt. Soc. Amer. B*, vol. 19, pp. 890–894, 2002.
[14] A. M. Afromowitz, "Refractive index of AlGaAs," *Solid State Commun.*, vol. 15, pp. 5–63, 1974.
[15] S. Adachi, "Refractive indexes of III-V compounds: key properties of InGaAsP relevant to device design," *J. Appl. Phys.*, vol. 53, pp. 5863–5869, 1982.
[16] M. M. Fejer, G. A. Magel, D. H. Jundt, and R. L. Byer, "Quasiphase-matched second harmonic-generation—tuning and tolerances," *IEEE J. Quantum Electron.*, vol. 28, no. 11, p. 2631, Nov. 1992.
[17] C. De Angelis, F. Gringoli, M. Midrio, D. Modotto, J. S. Aitchison, and G. F. Nalesso, "Conversion efficiency for second-harmonic generation in photonic crystals," *J. Opt. Soc. Amer. B*, vol. 18, p. 348, 2001.
[18] D. Modotto, private communication, 2001.
[19] O. P. Kowalski, C. J. Hamilton, S. D. McDougall, J. H. Marsh, A. C. Bryce, R. M. De la Rue, B. Vögele, and C. R. Stanley, "A universal damage induced technique for quantum well intermixing," *Appl. Phys. Lett.*, vol. 72, pp. 581–583, 1998.
[20] B. S. Ooi, Y. S. Tang, A. Saher Helmy, A. C. Bryce, J. H. Marsh, M. Paquette, and J. Beauvais, "Optical characterization of GaAs–AlGaAs quantum well wires fabricated using arsenic implantation induced intermixing," *J. Appl. Phys.*, vol. 83, pp. 4526–4530, 1998.
[21] J. P. Reithmaier and A. Forchel, "Focused ion-beam implantation induced thermal quantum-well intermixing for monolithic optoelectronic device integration," *IEEE J. Sel. Topics Quantum Electron.*, vol. 4, no. 4, pp. 595–605, Jul. 1998.
[22] J. P. Bouchard, M. Tetu, S. Janz, D.-X. Xu, Z. R. Wasilewski, P. Piva, U. G. Akano, and I. V. Mitchell, "Quasiphase matched second-harmonic generation in an AlxGa1$_x$As asymmetric quantum-well waveguide using ion-implantation-enhanced intermixing," *Appl. Phys. Lett*, vol. 77, pp. 4247–4249, 2000.
[23] M. W. Street, N. D. Whitebread, D. C. Hutchings, J. M. Arnold, J. H. Marsh, and J. S. Aitchison, "Quantum-well intermixing for the control of second-order nonlinear effects in AlGaAs multiple-quantum-well waveguides," *Opt. Lett.*, vol. 22, pp. 1600–1602, 1997.
[24] V. G. Litovchenko, D. V. Korbutyak, S. Krylyuk, H. T. Grahn, and K. H. Ploog, "Enhancement of electron-phonon interaction in ultrashort-period GaAs–AlAs superlattices," *Phys. Rev. B*, vol. 55, pp. 10 621–10 624, 1997.
[25] P. Dawson, "Optical properties of GaAs–AlAs type II quantum wells," *Opt. Quantum Electron.*, vol. 2, pp. S231–S242, 1990.
[26] G. Leo, C. Caldarella, G. Masini, A. D. Rossi, G. Assanto, O. Durand, M. Calligaro, X. Marcadet, and V. Berger, "X-ray and optical characterization of multilayer AlGaAs waveguides," *Appl. Phys. Lett*, vol. 77, pp. 3884–3886, 2000.
[27] M. L. Dakss, L. Kuhn, P. F. Heidrich, and B. A. Scott, "Grating coupler for efficient excitation of optical guided waves in thin films," *Appl. Phys. Lett*, vol. 16, pp. 523–525, 1970.
[28] R. G. Kaufman, G. R. Hulse, D. J. Vezetti, A. L. Moretti, K. A. Stair, G. P. Devane, and T. E. Bird, "Measurement of the refractive index of AlxGa1_xAs and the mode indicies of guided modes by a grating coupler technique," *J. Appl. Phys.*, vol. 75, pp. 8053–8059, 1994.
[29] P. Martin, E. M. Skouri, L. Chusseau, and C. Alibert, "Accurate refractive index measurements of doped and undoped InP by a grating coupler technique," *Appl. Phys. Lett.*, vol. 67, pp. 881–883, 1995.
[30] D. C. Hutchings, M. Sorel, K. Zeaiter, A. J. Zilkie, B. Leesti, A. Saher Helmy, P. W. E. Smith, and J. S. Aitchison, "Quasiphase-matched second harmonic generation with picosecond pulses in GaAs–AlAs superlattice waveguides," in *Nonlinear Guided Waves and their Applications*. Toronto, ON, Canada, 2004, pp. 881–883.
[31] P. Dumais, A. Villeneuve, A. Saher Helmy, J. S. Aitchison, L. Friedrich, R. A. Fuerst, and G. I. Stegeman, "Toward soliton emission in asymmetric GaAs–AlGaAs multiple-quantum-well waveguide structures below the half-bandgap," *Opt. Lett.*, vol. 25, pp. 1282–1285, 2000.

T. C. Kleckner received the B.Sc. degree in engineering physics (with distinction) from the University of Alberta, Edmonton, AL, CAnada, the M.A.Sc. degree from the Department of Electrical and Computer Engineering, University of British Columbia, Vancouver, BC, Canada, and the Ph.D. degree from the Department of Electronics and Electrical Engineering, University of Glasgow, Glasgow, U.K.

While at the University of Glasgow, his studies of second-order nonlinear effects in periodically disordered supperlattices were supported through the tenure of a Commonwealth Scholarship and a Natural Sciences and Engineering Research Council of Canada postgraduate scholarship. He is currently with the optical design software company Lumerical Solutions, Vancouver, which he co-founded in 2003.

A. S. Helmy (S'97–M'99) received the B.Sc.degree from Cairo University, Cairo, Egypt, in electronics and telecommunications engineering in 1993, the M.S. and Ph.D. degrees from the University of Glasgow, Glasgow, U.K., with a focus on photonic fabrication technologies, in 1999 and 1994, respectively.

He is an Assistant Professor in the Department of Electrical and Computer Engineering at the University of Toronto, Toronto, ON, Canada. Prior to his academic career, he held a position at Agilent Technologies Photonic Devices, Research and Development Division, Ipswich, U.K. At Agilent, his responsibilities included developing distributed feedback lasers, monolithically integrated lasers, modulators and amplifiers in InP-based semiconductors. He also developed high-powered submarine-class 980-nm InGaAs pump lasers. His research interests include photonic device physics and characterization techniques, with emphasis on nonlinear optics in III–V semiconductors; applied optical spectroscopy in III–V optoelectronic devices and materials; III–V fabrication and monolithic integration techniques.

Dr. Helmy is a member of IEEE LEOS and the Optical Society of America.

K. Zeaiter was born in Beirut, Lebanon. He received the M. Sc. (hons) in physics from Lebanese University Beirut, Lebanon, in 1995, the Postgraduate diploma in plasma-optoelectronics from Université Nancy I, Nancy, France, in 1996, and the Ph.D. (hons.) degree in condensed matter physics from Université Montpellier II, Monpellier, France, in 1999.

He worked for three years as Research Assistant at University of Glasgow, Glasgow, U.K. Currently, he is working as a Research Scientist at Spheral Solar Power, Cambridge, ON, Canada.

David C. Hutchings (M'98–SM'00) received the B.Sc. (hons) and Ph.D degrees in physics from Heriot-Watt University, Edinburgh, U.K., in 1984 and 1988, respectively.

He has held postdoctoral research positions at Heriot-Watt University and the Center for Research and Education in Optics and Lasers (CREOL), University of Central Florida, Orlando. He joined the Department of Electronics and Electrical Engineering at the University of Glasgow, Glasgow, U.K., in 1992 where he currently holds a personal chair in Optical and Quantum Electronics. He is currently Head of the Engineering Faculty Graduate School. He is the leading authority on ultrafast nonlinear optics in the transparency range in semiconductors. He also has research interests in solitons, integrated magneto-optics and computational electrodynamics and has authored over 60 journal articles.

Prof. Hutchings has held personal research fellowships from the Royal Society of Edinburgh/ Scottish Executive Enterprise and Lifelong Learning Department (1992–1995, 2003) and an advanced fellowship from the Engineering and Physical Sciences Research Council (1995–2000). He is a Fellow of the Institute of Physics.

J. S. Aitchison (M'96–SM'00) received the B.Sc. (first class hons.) and the Ph.D degrees from the Physics Department, Heriot-Watt University, Edinburgh, U.K., in 1984 and 1987, respectively. His dissertation research was on optical bistability in semiconductor waveguides.

From 1988 to 1990, he was a Postdoctoral Member of Technical Staff at Bellcore, Red Bank, NJ. His research interests were in high nonlinearity glasses and spatial optical solitons. He then joined the Department of Electronics and Electrical Engineering, University of Glasgow, Glasgow, U.K., in 1990 and was promoted to a Personal Chair as Professor of Photonics in 1999. His research was focused on the use of the half bandgap nonlinearity of III–V semiconductors for the realization of all-optical switching devices and the study of spatial soliton effects. He also worked on the development of quasi-phase matching techniques in III–V semiconductors, monolithic integration, optical rectification, and planar silica technology. His research group developed novel optical biosensors, waveguide lasers and photosensitive direct writing processes based around the use of flame hydrolysis deposited (FHD) silica. In 1996, he was the holder of a Royal Society of Edinburgh Personal Fellowship and carried out research on spatial solitons as a Visiting Researcher at Center for Research and Education in Optics and Lasers (CREOL), University of Central Florida, Orlando. He currently holds the Nortel Institute chair in Emerging Technology and is Director of the Emerging Communications Technology Institute at the University of Toronto. His research interests cover all-optical switching and signal processing, optoelectronic integration and optical bio-sensors. His research has resulted in seven patents, around 150 journal publications, and 200 conference publications.

Dr. Aitchison is a Fellow of the Optical Society of America and a Fellow of the Institute of Physics London.